JOURNAL OF GUIDANCE, CONTROL, AND DYNAMICS
Vol. 33, No. 3, May–June 2010

Noncertainty-Equivalent Adaptive Missile Control via Immersion and Invariance

Keum W. Lee*
University of Kwandong, Gangwon 210-701, Republic of Korea
and
Sahjendra N. Singh
University of Nevada, Las Vegas, Las Vegas, Nevada 89154-4026

DOI: 10.2514/1.47509

This paper presents a new noncertainty-equivalent adaptive control system for the control of a missile based on the immersion-and-invariance approach. The mathematical model of the missile represents the nonlinear longitudinal dynamics, and it is assumed that all the aerodynamic parameters (except the sign of a single control input gain) are not known. The objective here is to control the angle of attack of the missile. For the trajectory control of the angle of attack, a nonlinear noncertainty-equivalent adaptive control system is designed, and Lyapunov stability theory is used for stability analysis in the closed-loop system. The autopilot has a modular structure, which consists of a control module and a parameter estimator. In this noncertainty-equivalent adaptive law, each estimated parameter is the sum of a partial estimate generated by an update law and a nonlinear function. For comparison, a traditional certainty-equivalent adaptive control system is also designed. A special feature of the designed noncertainty-equivalent adaptive autopilot (unlike the certainty-equivalent adaptive systems) is that whenever the estimated parameters attain their true values, they remain frozen thereafter. Furthermore, it is shown that the trajectory of the closed-loop system, including the noncertainty-equivalent adaptive law, is eventually confined to a manifold in the space of missile states and estimated parameters, and the autopilot asymptotically recovers the performance of a deterministic control system. Simulation results for the noncertainty-equivalent adaptive and certainty-equivalent adaptive laws are presented. These results show that the designed autopilots accomplish trajectory control of the angle of attack despite uncertainties in the system parameters, but for properly chosen feedback and adaptation gains, the trajectory tracking performance is better with the noncertainty-equivalent adaptive law.

I. Introduction

MODERN aircraft and missiles often operate in a highly nonlinear regime in which the aerodynamic parameters have wide variations. For example, missiles must maneuver to intercept an agile, evading target. In the past, considerable effort has been made to develop guidance and control laws for missiles. For missile autopilot design, both the classical and modern design techniques have been applied. A survey of classical designs and modern designs based on linear quadratic Gaussian with loop transfer recovery (LQG/LTR) and eigenstructure assignment has been presented by Cloutier et al. [1]. Researchers have used gain scheduling and extended linearization for autopilot design [2–6]. Using extended linearization, a control law for a missile has been obtained, for which feedback gains are nonlinear functions of the Mach number and commanded angle of attack [6]. Of course, gain scheduling methods ignore the actual nonlinear behavior of the system.

In literature, a variety of nonlinear control methods have been proposed for missile autopilot design. Feedback linearization (dynamic inversion) approach has been used by several authors to design nonlinear flight control systems [7–11]. In this approach, the original nonlinear system is transformed into a linear system by coordinate transformation and feedback. Then for the linear model, a variety of linear design methods are applied to obtain suitable control systems. Of course, precise knowledge of system parameters is assumed for the derivation of control law by dynamic inversion. For the design of a robust missile autopilot, a combination of dynamic inversion and μ synthesis has been attempted [12]. The nonlinear H_∞ theory has been applied to missiles with coupled aerodynamic and thrust-vectoring control [13]. For the design of a nonlinear regulator of missiles, the state-dependent Riccati equation method has been considered [14,15]. For this, the nonlinear model is represented as a linearlike system, and a control law is obtained using a pointwise solution of the Riccati equation. This yields local stability in the closed-loop system [14]. Recently, a nonlinear missile autopilot design based on θ-D technique has been proposed. Using this method, an approximate solution of the Hamilton–Jacobi–Bellman equation is obtained and a suboptimal control law is synthesized [16,17].

For the control of missiles in the presence of uncertainties, sliding-mode control systems have been designed [18–22]. This approach gives a discontinuous control law. Adaptive control systems have been also developed for missiles with uncertain dynamics [23,24]. Using recently developed adaptive L_1 theory, an autopilot for a missile using output feedback has been derived [25]. For missiles with unstructured nonlinear dynamics, adaptive neural controllers have been proposed [26,27]. In the neural controller of [26], a certainty-equivalent adaptive law has been used. However, in certainty-equivalent adaptive (CEA) systems, the update law is a function of the tracking error and, as such, parameter adaptation never stops, even if the estimated parameters coincide with their true values at certain instants. Moreover, the update law of [26] requires modification using parameter projection method to avoid singularity in the control law. Recently, a new method for the design of adaptive control system for uncertain nonlinear systems based on immersion-and-invariance (I&I) theory has been developed [28–30]. This approach gives a noncertainty-equivalent adaptive (NCEA) law. Recently, the I&I approach has been used to develop NCEA control systems for a spacecraft [31] and an aeroelastic system [32].

The contribution of this paper lies in the derivation of a longitudinal autopilot for the control of a missile based on the immersion-and-invariance theory. The mathematical model of the missile includes nonlinearities, and it is assumed that the system parameters

Received 4 October 2009; revision received 4 January 2010; accepted for publication 4 January 2010.

*Division of Electronic Information and Communication.
†Department of Electrical and Computer Engineering; sahaj@egr.unlv.edu (Corresponding Author).

(except the sign of a single control input coefficient) are not known. The objective is to control the angle of the attack of the missile. Of course, this design approach can be also applied for the control of nonlinear state-dependent controlled output variables. For the trajectory tracking of the angle of attack, a noncertainty-equivalent adaptive control system is designed. The NCEA controller has a modular configuration, which consists of a control module and a separately designed parameter identifier. The estimate of each parameter is the sum of a partial estimate generated by an update law and a nonlinear function. Using Lyapunov stability theory, it is shown that in the closed-loop system, asymptotic trajectory control of the angle of attack is accomplished. A traditional CEA control system is also designed. Interestingly, unlike the traditional adaptive systems, the derived adaptation law freezes the parameter estimates whenever these estimates coincide with the true values. Moreover, the trajectories of the system with the NCEA law converge to a manifold, and on this manifold, the controller recovers the performance of a deterministic control system. This cannot happen in CEA control systems. Simulation results are presented that show that the NCEA autopilot accomplishes angle-of-attack trajectory control despite uncertainties in the aerodynamic parameters. These results also show that for properly chosen feedback and adaptation gains, the tracking-error control performance of the NCEA law is better than the CEA law.

II. Missile Longitudinal Dynamics and Control Problem

The mathematical model used in this paper is based on a tail-controlled missile. This model assumes constant mass: that is, after burnout, zero roll angle and roll rate, no sideslip, and zero yaw rate. Under these assumptions, the motion of the missile is described by two force equations and one kinematic equation. The complete equations of motion derived in [14] are given by

$$\begin{aligned}\dot{M} &= (-0.7P_0S/ma)[M^2(C_{D_0} - C_N\sin\alpha)] - (g/a)\sin\gamma\\ \dot{\alpha} &= (0.7P_0S/ma)MC_N\cos\alpha + (g/aM)\cos\gamma + Q\\ \dot{Q} &= (0.7P_0Sd/I_Y)M^2C_m \qquad \dot{\theta} = Q\end{aligned} \tag{1}$$

where the state variables are Mach number M, angle of attack α, pitch rate Q, and pitch angle θ; $\gamma = \theta - \alpha$ is the flight-path angle; P_0 is the static pressure; I_Y is the moment of inertia; m is the mass; S is the reference area; a is the speed of sound; g is the gravity; and C_{D_0}, C_N, and C_m are nondimensional aerodynamic coefficients. For the missile at 20,000 ft altitude, the aerodynamic coefficients are $C_{D_0} = 0.3$ and

$$\begin{aligned}C_N &= a_n\alpha^3 + b_n\alpha|\alpha| + c_n(2 - (M/3))\alpha + d_n\delta\\ C_m &= a_m\alpha^3 + b_m\alpha|\alpha| + c_m(-7 - (8M/3))\alpha + d_m\delta + e_mQ\end{aligned}$$

where δ is the control surface deflection and a_k, b_k, d_k, and e_k are constant parameters.

For the mass properties and the aerodynamic coefficients given in [14], the dynamic equations are given by

$$\begin{aligned}\dot{\alpha} &= 0.4008M\alpha^3\cos\alpha - 0.6419M|\alpha|\alpha\cos(\alpha)\\ &\quad - 0.2010M\left(2 - \frac{M}{3}\right)\alpha\cos(\alpha) + 0.0311\frac{\cos(\theta-\alpha)}{M}\\ &\quad + Q - 0.0403M\cos\alpha\cdot\delta \triangleq p_1^T\phi_1(M,\alpha,\theta)\\ &\quad + Q + b_{01}M\cos\alpha\cdot\delta\end{aligned} \tag{2}$$

$$\begin{aligned}\dot{M} &= p_1^T[M^2\alpha^3\sin\alpha, M^2|\alpha|\alpha\sin\alpha, M^2\left(2 - \frac{M}{3}\right)\alpha\sin\alpha,\\ &\quad - \sin(\theta-\alpha)]^T - 0.0062M^2 - 0.0403M^2\sin\alpha\\ &\quad\cdot\delta \triangleq p_1^T\phi_2(M,\alpha,\theta) + r_1M^2 + b_{02}M^2\sin\alpha\cdot\delta\end{aligned} \tag{3}$$

$$\begin{aligned}\dot{Q} &= 49.82M^2\alpha^3 - 78.86M^2|\alpha|\alpha + 3.6M^2\left(-7 - \frac{8M}{3}\right)\alpha\\ &\quad - 2.12M^2Q - 14.54M^2\delta \triangleq p_3^T\phi_3(M,\alpha)\\ &\quad + r_2M^2Q + b_{03}M^2\delta\end{aligned} \tag{4}$$

where $b_{01} = -0.0403$, $r_1 = -0.0062$, $b_{02} = -0.0403$, $r_2 = -2.12$, $b_{03} = -14.54$, the regressor vectors are

$$\phi_1 = \left[M\alpha^3\cos\alpha, M|\alpha|\alpha\cos\alpha, M\left(2-\frac{M}{3}\right)\alpha\cos\alpha, \frac{\cos(\theta-\alpha)}{M}\right]^T \in R^4$$

$$\phi_2 = \left[M^2\alpha^3\sin\alpha, M^2|\alpha|\alpha\sin\alpha, M^2\left(2-\frac{M}{3}\right)\alpha\sin\alpha, -\sin(\theta-\alpha)\right]^T \in R^4$$

$$\phi_3 = \left[M^2\alpha^3, M^2|\alpha|\alpha, M^2\left(-7-\frac{8M}{3}\right)\alpha\right]^T \in R^3$$

and the parameter vectors are

$$\begin{aligned}p_1 &= (0.4008, -0.6419, -0.2010, 0.0311)^T\\ &= (p_{11}, p_{12}, p_{13}, p_{14})^T \in R^4\\ p_3 &= (49.82, -78.86, 3.6)^T = (p_{31}, p_{32}, p_{33})^T \in R^3\end{aligned}$$

Let the kth element of ϕ_i be ϕ_{ik}, $(i = 1, 2, 3)$.

Defining the state vector $x = (\alpha, M, Q, \theta)^T \in R^4$, the missile dynamics can be written as

$$\dot{x} = \begin{bmatrix}\phi_1^T(\alpha,M,\theta)p_1 + Q\\ \phi_2^T(\alpha,M,\theta)p_1 + r_1M^2\\ \phi_3^T(\alpha,M)p_3 + r_2M^2Q\\ Q\end{bmatrix} + \begin{bmatrix}b_{01}M\cos\alpha\\ b_{02}M^2\sin\alpha\\ b_{03}M^2\\ 0\end{bmatrix}\delta \tag{5}$$

Let the controlled output variable be

$$y = \alpha \tag{6}$$

It is assumed that all the parameter vectors p_k $(k = 1, 2, 3)$, r_1, r_2, b_{01}, and b_{02} are unknown, but we make the following assumption.

Assumption 1: The magnitude of b_{03} is unknown, but its sign is known.

In this paper, trajectory control of the angle of attack is considered. Suppose that a reference angle-of-attack trajectory $y_r = \alpha_r(t)$ is given. Of course, an autopilot command logic can be used to convert commanded normal acceleration from the guidance laws to reference angle-of-attack commands for the autopilot. Such an approach has been also adopted in [17]. We are interested in deriving an adaptive control law such that in the closed-loop system, the angle of attack α asymptotically tracks α_r in spite of the uncertainties in the missile parameters.

III. Adaptive Control System Design

In this section, design of a noncertainty-equivalent adaptive control system based on the I&I theory is considered. The I&I approach provides a control system, which has a modular structure consisting of 1) a control module and 2) an identifier. The designs of the control module and the identifier are done separately. Unlike the traditional adaptive design method, the identifier provides an estimate of unknown parameter, which is a sum of a partial estimate generated by an update law and a judiciously chosen nonlinear function. The essential idea of the I&I method is to create a manifold that is invariant in the extended space of missile states and partial parameter estimates. The trajectories beginning on this manifold remain confined to it for all future time. As the trajectory evolves on this invariant manifold, the closed-loop system captures the behavior of a target system, which can be obtained by synthesizing a full-information feedback (deterministic) control law. The nonlinear function in the parameter estimate allows construction of estimation error dynamics (off-the-invariant manifold dynamics) that have

stable zero equilibrium. (Later, Remarks 1 and 2 provide precise statements related to the invariant manifold and performance recovery.)

For the design of the autopilot, a simplified model of the missile is considered. Since the control surface is principally a moment-producing device, the small force generated by it will be ignored. Therefore, we set b_{01} and b_{02} to zero for the derivation of control system, but for the evaluation of controller, nonzero values of b_{01} and b_{02} will be retained.

First note that Eq. (2) (with $b_{01} = 0$) gives

$$Q = \dot{\alpha} - p_1^T \phi_1 = \dot{\theta} \tag{7}$$

Then substituting for Q in Eq. (4) yields

$$\begin{aligned}\dot{Q} &= p_3^T \phi_3 + r_2 M^2 [\dot{\alpha} - p_1^T \phi_1] + b_{03} M^2 \delta \\ &= [p_3^T, r_2, -r_2 p_1^T] \begin{bmatrix} \phi_3 \\ M^2 \dot{\alpha} \\ M^2 \phi_1 \end{bmatrix} \\ &\quad + b_{03} M^2 \delta \triangleq p_4^T \phi_4(M, \alpha, \dot{\alpha}, \theta) + b_{03} M^2 \delta \end{aligned} \tag{8}$$

where $p_4 = [p_3^T, r_2, -r_2 p_1^T]^T \in R^8$ and

$$\phi_4 = \begin{bmatrix} \phi_3 \\ M^2 \dot{\alpha} \\ M^2 \phi_1 \end{bmatrix} \in R^8$$

For feedback-linearizing control of the angle of attack, we differentiate α until the control input δ appears. Of course, we have assumed that b_{01} and b_{02} are zero. Thus, using Eq. (3) (with $b_{02} = 0$) and Eq. (7), the second derivative of α takes the form

$$\begin{aligned}\ddot{\alpha} &= p_1^T \dot{\phi}_1 + \dot{Q} = p_1^T \left[\frac{\partial \phi_1}{\partial M} \dot{M} + \frac{\partial \phi_1}{\partial \alpha} \dot{\alpha} + \frac{\partial \phi_1}{\partial \theta} \dot{\theta} \right] + \dot{Q} \\ &= p_1^T \frac{\partial \phi_1}{\partial M} [p_1^T \phi_2 + r_1 M^2] + p_1^T \frac{\partial \phi_1}{\partial \alpha} \dot{\alpha} + p_1^T \frac{\partial \phi_1}{\partial \theta} [\dot{\alpha} - p_1^T \phi_1] \\ &\quad + (p_4^T \phi_4 + b_{03} M^2 \delta) \end{aligned} \tag{9}$$

Collecting terms, Eq. (9) can be written as

$$\begin{aligned}\ddot{\alpha} &= [p_1^T r_1, p_1^T, p_4^T] \begin{bmatrix} \frac{\partial \phi_1}{\partial M} M^2 \\ \left(\frac{\partial \phi_1}{\partial \alpha} + \frac{\partial \phi_1}{\partial \theta} \right) \dot{\alpha} \\ \phi_4 \end{bmatrix} + f_n + b_{03} M^2 \delta \\ &\triangleq p_a^T \phi_a(M, \alpha, \dot{\alpha}, \theta) + f_n + b_{03} M^2 \delta \end{aligned} \tag{10}$$

where the nonlinear function is

$$f_n = \left[\frac{\partial \phi_1^T}{\partial M} p_1 p_1^T \phi_2 - \frac{\partial \phi_1^T}{\partial \theta} p_1 p_1^T \phi_1 \right]$$

$p_a = [p_1^T r_1, p_1^T, p_4^T]^T \in R^{16}$, and ϕ_a is defined in Eq. (10). Since $p_1 p_1^T$ is a symmetric 4×4 unknown matrix, it has 10 distinct parameters. Therefore, the function f_n can be linearly parameterized as

$$f_n = \phi_b^T p_b \tag{11}$$

where the parameter vector $p_b \in R^{10}$ is

$$p_b = [p_{11}^2, p_{11}p_{12}, p_{11}p_{13}, p_{11}p_{14}, p_{12}^2, p_{12}p_{13}, p_{12}p_{14}, p_{13}^2, p_{13}p_{14}, p_{14}^2]^T$$

and the nonlinear vector function ϕ_b is given by

$$\phi_b = [\phi_{ba} - \phi_{bc}, \phi_{bb} - \phi_{bd}]^T$$

The functions ϕ_{bq} for $q \in \{a, b, c, d\}$ are

$$\begin{aligned}\phi_{ba} &= \left[\frac{\partial \phi_{11}}{\partial M} \phi_{21}, \frac{\partial \phi_{11}}{\partial M} \phi_{22} + \frac{\partial \phi_{12}}{\partial M} \phi_{21}, \frac{\partial \phi_{11}}{\partial M} \phi_{23} + \frac{\partial \phi_{13}}{\partial M} \phi_{21}, \frac{\partial \phi_{11}}{\partial M} \phi_{24} \right. \\ &\quad \left. + \frac{\partial \phi_{14}}{\partial M} \phi_{21}, \frac{\partial \phi_{12}}{\partial M} \phi_{22} \right] \\ \phi_{bb} &= \left[\frac{\partial \phi_{12}}{\partial M} \phi_{23} + \frac{\partial \phi_{13}}{\partial M} \phi_{22}, \frac{\partial \phi_{12}}{\partial M} \phi_{24} + \frac{\partial \phi_{14}}{\partial M} \phi_{22}, \frac{\partial \phi_{13}}{\partial M} \phi_{23}, \frac{\partial \phi_{13}}{\partial M} \phi_{24} \right. \\ &\quad \left. + \frac{\partial \phi_{14}}{\partial M} \phi_{23}, \frac{\partial \phi_{14}}{\partial M} \phi_{24} \right] \\ \phi_{bc} &= \left[\frac{\partial \phi_{11}}{\partial \theta} \phi_{11}, \frac{\partial \phi_{11}}{\partial \theta} \phi_{12} + \frac{\partial \phi_{12}}{\partial \theta} \phi_{11}, \frac{\partial \phi_{11}}{\partial \theta} \phi_{13} + \frac{\partial \phi_{13}}{\partial \theta} \phi_{11}, \frac{\partial \phi_{11}}{\partial \theta} \phi_{14} \right. \\ &\quad \left. + \frac{\partial \phi_{14}}{\partial \theta} \phi_{11}, \frac{\partial \phi_{12}}{\partial \theta} \phi_{12} \right] \\ \phi_{bd} &= \left[\frac{\partial \phi_{12}}{\partial \theta} \phi_{13} + \frac{\partial \phi_{13}}{\partial \theta} \phi_{12}, \frac{\partial \phi_{12}}{\partial \theta} \phi_{14} + \frac{\partial \phi_{14}}{\partial \theta} \phi_{12}, \frac{\partial \phi_{13}}{\partial \theta} \phi_{13}, \frac{\partial \phi_{13}}{\partial \theta} \phi_{14} \right. \\ &\quad \left. + \frac{\partial \phi_{14}}{\partial \theta} \phi_{13}, \frac{\partial \phi_{14}}{\partial \theta} \phi_{14} \right] \end{aligned}$$

Substituting Eq. (11) in Eq. (10), one obtains

$$\ddot{\alpha} = p_a^T \phi_a + p_b^T \phi_b + b_{03} M^2 \delta \tag{12}$$

Consider a change of control input variable given as

$$M^2 \delta = \operatorname{sgn}(b_{03}) u \tag{13}$$

where u is a new input. Defining $b_1 = |b_{03}| > 0$ and a parameter vector

$$w_1 = [p_a^T, p_b^T]^T \in R^{26}$$

Eq. (12) can be written as

$$\ddot{\alpha} = \Psi^T(\alpha, \dot{\alpha}, M, \theta) w_1 + b_1 u \tag{14}$$

where $\Psi(\alpha, \dot{\alpha}, M, \theta) = [\phi_a^T, \phi_b^T]^T \in R^{26}$. For the derivation of control-law equation (14) will be used.

A. NCEA Control Module

Now the derivation of the NCEA law is considered. Since the parameter vector w_1 and b_1 are unknown, their estimates are needed for synthesis. Let the estimates of w_1 and $w_2 = b_1^{-1}$ be $\hat{w}_1 + \mu_1$ and $\hat{w}_2 + \mu_2$, respectively, where μ_i are nonlinear functions to be determined later. One can think of $\hat{w}_i$ as only a partial estimate of w_i, and the full estimate of parameters is obtained by combining the nonlinear function μ_i with $\hat{w}_i$. This is an important difference from the estimates used in CEA laws. In CEA laws, $\mu_i = 0$, and only an update law for $\hat{w}_i$ is sufficient. The introduction of nonlinear functions μ_i in the parameter identifier enhances stability in the closed-loop system. Let the parameter errors be

$$z_1 = \hat{w}_1 + \mu_1 - w_1 \qquad z_2 = \hat{w}_2 + \mu_2 - w_2 \tag{15}$$

Since the interest is in tracking α_r, consider a surface defined as

$$s_1 = \dot{\tilde{\alpha}} + \lambda \tilde{\alpha} = 0 \tag{16}$$

where $\tilde{\alpha} = \alpha - \alpha_r$ is the tracking error and $\lambda > 0$. It is assumed that $\dot{\alpha}$ is measured for feedback. If s_1 is zero, then it follows that the tracking error converges to zero. As such, it is sufficient to design a control law that forces s_1 to zero.

Using Eq. (16), the derivative of s_1 can be written as

$$\dot{s}_1 = (\Psi^T w_1 + b_1 u) - \ddot{\alpha}_r + \lambda \dot{\tilde{\alpha}} \tag{17}$$

We select a control input u as

$$u = (\hat{w}_2 + \mu_2) v \tag{18}$$

where v is a new input yet to be determined. Note that

$$b_1 u = b_1(\hat{w}_2 + \mu_2)v = b_1(z_2 + w_2)v$$
$$= b_1(z_2 + b_1^{-1})v = b_1 z_2 v + v \tag{19}$$

which can be substituted in Eq. (17) to give

$$\dot{s}_1 = \Psi^T(\hat{w}_1 + \mu_1 - z_1) + v + b_1 z_2 v - \ddot{\alpha}_r + \lambda\dot{\tilde{\alpha}} \tag{20}$$

Now in view of Eq. (20), the control input v is chosen to stabilize the tracking-error dynamics. For this, v is selected as

$$v(\alpha, \dot{\alpha}, M, \hat{w}_1, \theta, \mu_1, t) = -[\Psi^T(\alpha, \dot{\alpha}, M, \theta)(\hat{w}_1 + \mu_1) + c_1 s_1 - \ddot{\alpha}_r + \lambda\dot{\tilde{\alpha}}] \tag{21}$$

where the gain $c_1 > 0$ and the argument t denotes the dependence of v on α_r and its derivatives. The control law has been chosen to cancel estimated functions. Now v from Eq. (21) is substituted in Eq. (20) to obtain

$$\dot{s}_1 = -\Psi^T z_1 - c_1 s_1 + b_1 z_2 v = -c_1 s_1 - \Psi_s^T(\alpha, \alpha_r, M, \theta, v)z \tag{22}$$

where $z = (z_1^T, z_2)^T \in R^{27}$ and $\Psi_s = [\Psi^T, -b_1 v]^T \in R^{27}$.

For examining the stability property of s_1, consider a Lyapunov function

$$V_1 = s_1^2 \tag{23}$$

Differentiating V_1 along the solution of Eq. (22) gives

$$\dot{V}_1 = 2s_1\dot{s}_1 = 2s_1(-c_1 s_1 - \Psi_s^T z) = -2c_1 s_1^2 - 2s_1\Psi_s^T z \tag{24}$$

By Young's inequality, one has

$$-2s_1\Psi_s^T z \le c_1 s_1^2 + c_1^{-1}(\Psi_s^T z)^2 \tag{25}$$

Then using inequality Eq. (25) in Eq. (24) gives

$$\dot{V}_1 \le -c_1 s_1^2 + c_1^{-1}(\Psi_s^T z)^2 \tag{26}$$

We observe from Eq. (27) that if $\Psi_s^T z$ is bounded, then s_1 will be bounded. This in turn will imply boundedness of the tracking error. In the next section, a parameter estimator is designed that has the desirable property.

B. Parameter Estimator

Now the design of the parameter estimator is considered. This design is completed by deriving the adaptation law for the partial estimates $\hat{w}_i$ and the nonlinear functions μ_i. For the derivation, it is assumed that $\dot{M}$ and $\dot{\alpha}$ are available for feedback. Note that although this assumption is not necessary for the application of the immersion-and-invariance approach, one will need to solve a partial differential equation, which is not easily solvable if $\dot{M}$ and $\dot{\alpha}$ are not measured.

First note that using Eq. (19) in Eq. (14) gives

$$\ddot{\alpha} = \Psi^T(\alpha, \dot{\alpha}, M, \theta)w_1 + v + b_1 z_2 v \tag{27}$$

The vector μ chosen here is a function of $x_a = (\alpha, \dot{\alpha}, M, \theta)$, $\hat{w}$, and α_r. For the derivation, consider the parameter error dynamics obtained by differentiating z. Its derivative is

$$\dot{z} = \dot{\tilde{w}} + \frac{\partial\mu}{\partial\hat{w}}\dot{\hat{w}} + \frac{\partial\mu}{\partial\alpha}\dot{\alpha} + \frac{\partial\mu}{\partial M}\dot{M} + \frac{\partial\mu}{\partial\theta}\dot{\theta} + \frac{\partial\mu}{\partial\dot{\alpha}}[\Psi^T w_1 + v + b_1 z_2 v] + \frac{\partial\mu}{\partial t} \tag{28}$$

where $\hat{w} = (\hat{w}_1^T, \hat{w}_2)^T \in R^{27}$, $\mu = (\mu_1^T, \mu_2)^T \in R^{27}$, and $\partial\mu/\partial t$ denotes the terms arising from the dependence of μ on $\alpha_r(t)$ and its derivatives. In Eq. (28), $\dot{M}$ and $\dot{\alpha}$ are treated as known functions.

In view of Eq. (28), the update law is chosen as

$$\dot{\hat{w}} = -\left(I_{27\times 27} + \frac{\partial\mu}{\partial\hat{w}}\right)^{-1}\left[\frac{\partial\mu}{\partial\alpha}\dot{\alpha} + \frac{\partial\mu}{\partial M}\dot{M} + \frac{\partial\mu}{\partial\theta}Q + \frac{\partial\mu}{\partial\dot{\alpha}}\{\Psi^T(\hat{w}_1 + \mu_1) + v\} + \frac{\partial\mu}{\partial t}\right] \tag{29}$$

Substituting Eq. (29) in Eq. (28) gives

$$\dot{z} = -\frac{\partial\mu}{\partial\dot{\alpha}}[\Psi^T z_1 - b_1 z_2 v] = -\frac{\partial\mu}{\partial\dot{\alpha}}\Psi_s^T z \tag{30}$$

The nonlinear functions μ_i are chosen so that z dynamics have stable behavior. For this, one chooses

$$\frac{\partial\mu_1}{\partial\dot{\alpha}} = \gamma_1\Psi \in R^{26}, \qquad \frac{\partial\mu_2}{\partial\dot{\alpha}} = -\gamma_2 v \in R \tag{31}$$

where $\gamma_i > 0$. These equations are integrated to obtain μ_i. Thus, one has

$$\mu_1 = \int_0^{\dot{\alpha}} \gamma_1\Psi(\alpha, \chi, M, \theta)\,\mathrm{d}\chi \tag{32}$$

Now μ_1 is substituted in v [Eq. (21)]. Substituting μ_1 from Eq. (32) in Eq, (21), the signal v is obtained. Now Eq. (31) is integrated to obtain μ_2. It turns out that the matrix $\partial\mu/\partial\hat{w}$ is a lower triangular matrix with zero entry in the diagonal, and therefore Eq. (29) is always solvable.

Define a positive-definite diagonal matrix

$$\Gamma = \mathrm{diag}\{I_{26\times 26}\gamma_1, \gamma_2 b_1^{-1}\}$$

Then using Eq. (31) in Eq. (30), one obtains the z dynamics in a compact form given by

$$\dot{z} = -\Gamma\Psi_s(x_a, \hat{w}_1, t)\Psi_s^T(x_a, \hat{w}_1, t)z \tag{33}$$

To examine the stability property of the error dynamics, consider a positive-definite Lyapunov function $V_2(z)$:

$$V_2(z) = c_1^{-1} z^T\Gamma^{-1} z \tag{34}$$

Differentiating V_2 and using Eq. (33) gives

$$\dot{V}_2 = -2c_1^{-1} z^T\Psi_s\Psi_s^T z \le 0 \tag{35}$$

Since the derivative of V_2 is negative semidefinite, $z \in L_\infty[0, \infty)$ (the set of bounded functions) and the origin $z = 0$ is uniformly globally stable. Also integrating Eq. (23) gives

$$2c_1^{-1}\int_0^\infty (\Psi_s^T z)^2\,\mathrm{d}t = -V_2(z(\infty)) + V_2(z(0)) \le V_2(z(0))$$

which implies that $\Psi_s^T z \in L_2[0, \infty)$ (the set of square integrable functions).

Now we examine the stability property of the complete system equation (17) together with the update-law equation (29). For the stability analysis of the closed-loop system, consider the composite Lyapunov function $V = V_1 + V_2$. Differentiating V and using Eqs. (17) and (33), one obtains

$$\dot{V} \le -c_1 s_1^2 - c_1^{-1}(\Psi_s^T(x_a, \hat{w}_1, t)z)^2 \le 0 \tag{36}$$

Since V is a positive-definite function of s_1 and z, and $\dot{V} \le 0$, one finds that s_1 and z are bounded. Integrating Eq. (36), one finds that s_1 is square integrable. Of course, α and its derivative are bounded if s_1 is bounded. If the maneuvers are such that M and θ remain bounded, then Eq. (7) implies boundedness of Q. Since all signals are bounded, the derivatives of s_1 and $\Psi_s^T z$ are bounded. Therefore, according to Barbalat's lemma (see [33]), the tracking error and $\Psi_s^T z$ converge to zero.

Of course, in this derivation, a simplified model of the missile has been used. In the next section, simulation results are obtained for the

complete model (b_{01} and b_{02} nonzero). In the presence of unmodeled terms, an estimator parameter can diverge. However, divergence of parameter estimates can be avoided by modifying the update law using σ modification, if it is required.

To this end, we summarize the special features of the derived control law.

Remark 1: According to Eq. (33), the z dynamics can be treated as a linear time-varying system given as

$$\dot{z} = A(t)z \tag{37}$$

where

$$A(t) = -\Gamma\Psi_s(x_a(t), \hat{w}(t), t)\Psi_s^T(x_a(t), \hat{w}(t), t)$$

In view of Eq. (37), one notes that if at some instant t_1, $z(t_1) = 0$, then $z(t) = 0$ for $t \geq t_1$; that is, the manifold defined by

$$M_z = \{(x_a, \hat{w}, t) \in R^4 \times R^{27} \times R\text{: } \hat{w} + \mu - w = 0\}$$

is an invariant manifold. As such, the parameter vector estimate $\hat{w} + \mu$ remains frozen at its actual value for $t \geq t_1$. On this invariant manifold, one observes from Eq. (22) that $\dot{s}_1 = 0$, which can be obtained if a full-information feedback-linearizing control law is synthesized.

Remark 2: The origin $z = 0$ of the z dynamics equation (33) is uniformly stable, and the trajectory of the closed-loop system eventually resides in the manifold defined by

$$\Omega = \{(x_a, \hat{w}, t) \in R^4 \times R^{27} \times R\text{: } \Psi_s(x_a, \hat{w}_1, t)^T \times (\hat{w} + \mu(x, \hat{w}, t) - w) = 0\} \tag{38}$$

Consequently, in view of Eq. (22), $\dot{s}_1 = 0$; therefore, the closed-loop system asymptotically recovers the performance of a feedback-linearizing deterministic control law designed for known parameters. It is important to note that convergence of the function $\Psi_s^T z$ to zero does not imply convergence of the parameter error z to the null vector.

The adaptive law has several parameters for tuning, and the complexity of the controller increases with the number of unknown parameters. But modern computing devices can fulfil the computational need. For the synthesis of the designed controller, it is assumed here that not only the state variables, but also the derivatives of M and α, are available for feedback. Of course, synthesis of controllers using state feedback has been considered in literature (for example, [7,8,17]). Although one cannot measure $\dot{M}$ and $\dot{\alpha}$ directly, these could be generated by digital differentiation of M and α. Of course, differentiation of signals in the presence of noise is not preferable. Alternatively, one could attempt to compute $\dot{M}$ and $\dot{\alpha}$ using the relations

$$\dot{M} = (\dot{U}U + \dot{W}W)/\{2a(U^2 + W^2)^{1/2}\}$$
$$\dot{\alpha} = (\dot{W}U - W\dot{U})/(U^2\sec^2\alpha)$$

where U and W are the velocity components of the missile along the longitudinal and normal axes. The derivatives of U and W can be determined from $\dot{U} = -QW + a_{x_b}$ and $\dot{W} = UQ + a_{z_b}$, where a_{x_b} and a_{z_b} are the components of the inertial acceleration of the missile resolved along the longitudinal and normal axes.

IV. Certainty-Equivalent Adaptive Control Law

For the purpose of comparison, a certainty-equivalent adaptive control system is briefly presented in this section.

Let $\hat{w}_1$ and $\hat{w}_2$ be the estimates of w_1 and $w_2 = b_1^{-1}$; that is, now the nonlinear functions are $\mu_i = 0$ $(i = 1, 2)$. Define the parameter errors as

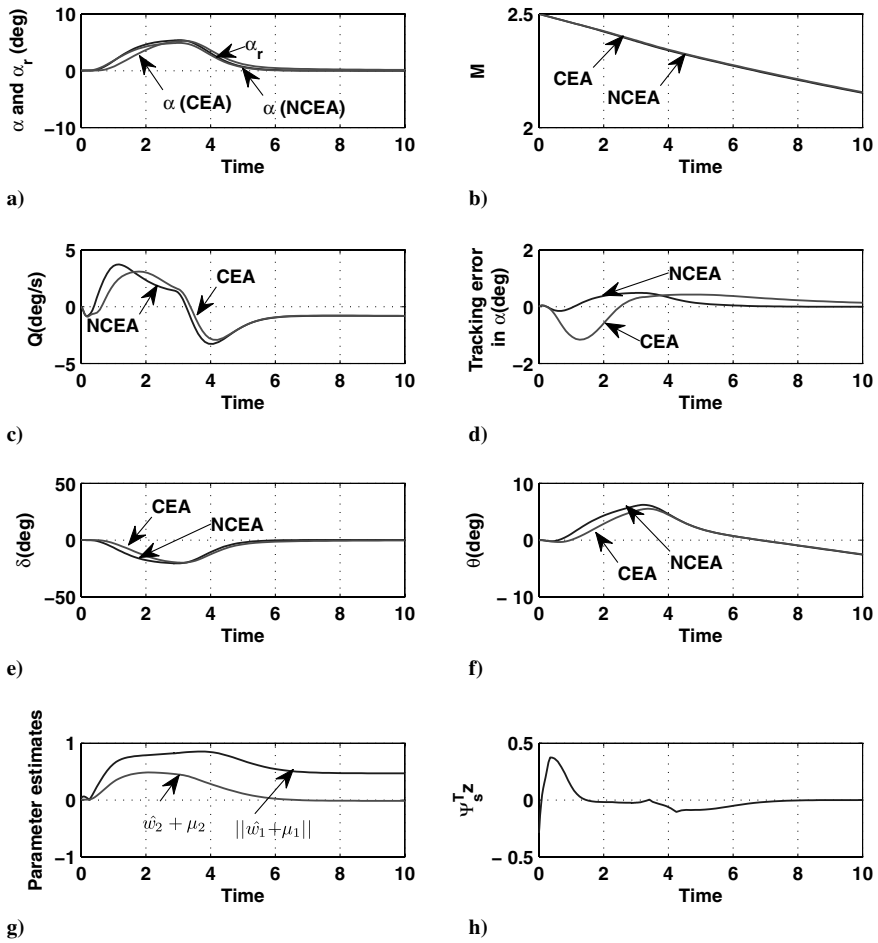

Fig. 1 Adaptive control for slow and small α_r command: $\rho_1 = 1$, $\rho_2 = 1$, $\omega_1 = 3$, $\omega_2 = 3$, $\alpha_r* \in \{5, 0\}$ deg.

$$z_1 = \hat{w}_1 - w_1, \qquad z_2 = \hat{w}_2 - w_2 \tag{39}$$

We select a control input u as

$$u = \hat{w}_2 v \tag{40}$$

where v is a new input yet to be determined. Note that

$$b_1 u = b_1 \hat{w}_2 v = b_1(z_2 + w_2)v = b_1(z_2 + b_1^{-1})v = b_1 z_2 v + v \tag{41}$$

which can be substituted in Eq. (17) to give

$$\dot{s}_1 = \Psi^T(\hat{w}_1 - z_1) + v + b_1 z_2 v - \ddot{\alpha}_r + \lambda\dot{\tilde{\alpha}} \tag{42}$$

Now in view of Eq. (42), the control input v is selected as

$$v(\alpha, \dot{\alpha}, M, \hat{w}_1, \theta, t) = -[\Psi^T(\alpha, \dot{\alpha}, M, \theta)\hat{w}_1 + c_1 s_1 - \ddot{\alpha}_r + \lambda\dot{\tilde{\alpha}}] \tag{43}$$

for stabilizing the tracking-error dynamics, where the gain $c_1 > 0$. Substituting the control-law Eq. (43) in Eq. (42) gives

$$\dot{s}_1 = -c_1 s_1 - \Psi^T(x) z_1 + b_1 z_2 v \tag{44}$$

Consider a Lyapunov function

$$W = s_1^2 + \gamma_1^{-1} z_1^T z_1 + b_1 \gamma_2^{-1} z_2^2 \tag{45}$$

Differentiating W gives

$$\dot{W} = 2s_1\dot{s}_1 + 2\gamma_1^{-1} z_1^T \dot{z}_1 + 2b_1\gamma_2^{-1} z_2 \dot{z}_2 \tag{46}$$

Substituting Eq. (44) in Eq. (46) and noting that $\dot{z}_1 = \dot{\hat{w}}_1$ and $\dot{z}_2 = \dot{\hat{w}}_2$ gives

$$\begin{aligned}\dot{W} &= 2s_1[-c_1 s_1 - \Psi^T(x) z_1 + b_1 z_2 v] + 2\gamma_1^{-1} z_1^T \dot{z}_1 \\ &\quad + 2b_1\gamma_2^{-1} z_2 \dot{z}_2 = -2c_1 s_1^2 + 2z_1^T[-s_1\Psi(x) + \gamma_1^{-1}\dot{\hat{w}}_1] \\ &\quad + 2b_1 z_2(s_1 v + \gamma_2^{-1}\dot{\hat{w}}_2)\end{aligned} \tag{47}$$

Now in view of Eq. (47), one selects the adaptation law of the form

$$\dot{\hat{w}}_1 = \gamma_1 \Psi(x) s_1, \qquad \dot{\hat{w}}_2 = -\gamma_2 v s_1 \tag{48}$$

Using Eq. (48) in Eq. (47) gives

$$\dot{W} = -2c_1 s_1^2 \tag{49}$$

Since W is a positive-definite function of s_1 and z, and $\dot{W}$ is negative semidefinite, it follows that s_1 and z_i are bounded and, furthermore, that s_1 is a square integrable function. Following the arguments similar to those of the previous section, one establishes the convergence of s_1 and the tracking error to zero.

We point out two important differences in this CEA law. Unlike the NCEA law of the previous section, the derivative of the Lyapunov function equation (49) does not have an additional nonnegative function $(\Psi_s^T z)^2$ present in Eq. (36). As such, the special feature of the NCEA law described in Remark 2 is not possible for the CEA law derived in this section. Furthermore, Remark 1 does not hold as well for the CEA system.

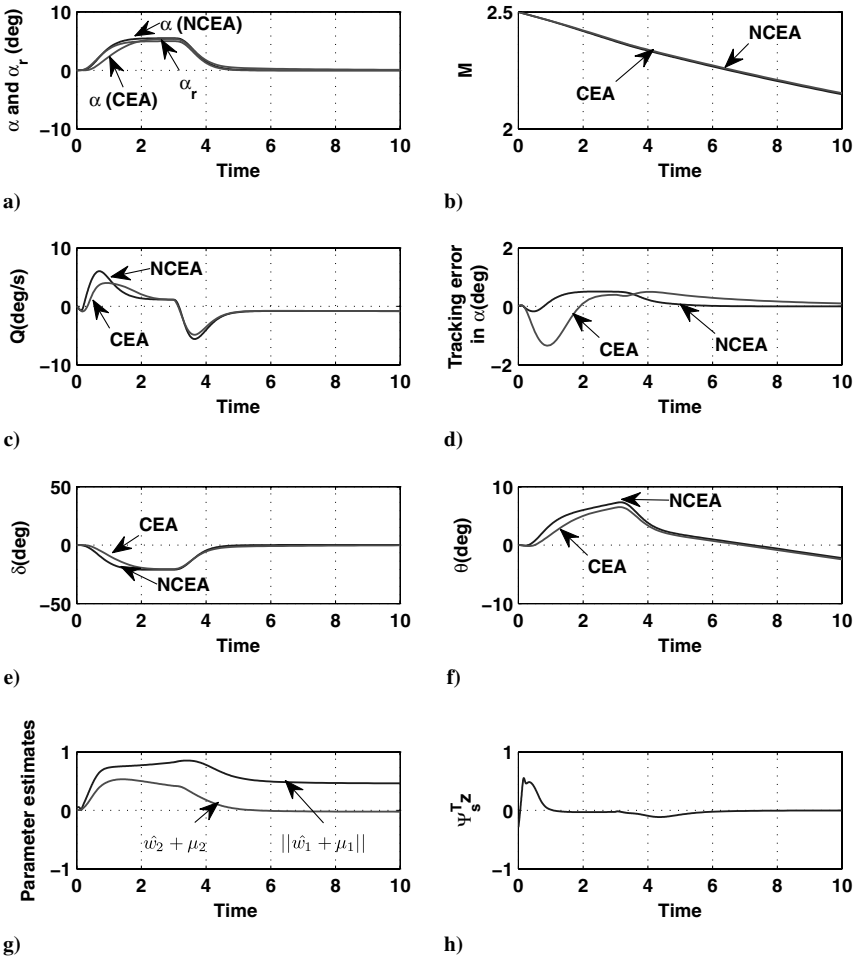

Fig. 2 Adaptive control for fast but small α_r command: $\rho_1 = 1$, $\rho_2 = 1$, $\omega_1 = 5$, $\omega_2 = 5$, and $\alpha_r* \in \{10, 0\}$ deg.

V. Simulation Results

This section presents the results of digital simulation for the closed-loop systems including the NCEA and CEA laws. The missile parameters of [14] are used for computation. The δ-dependent functions in $\dot{M}$ and $\dot{\alpha}$, which have been neglected for control-law derivation, are retained in the model for a realistic simulation (i.e. b_{10} and b_{20} are nonzero). The initial conditions of missile state variables are assumed to be $x(0) = [0, 2.5, 0, 0]^T$. For simulation, offnominal values of estimated parameters $\hat{w}_i(0) = 0$ $(i = 1, 2)$ are assumed. This is the worst choice of initial estimates of the parameters, but it has been made to examine the robustness of the control system. The reference trajectory α_r is generated by a fourth-order command generator of the form

$$(D^2 + 2\rho_1\omega_1 D + \omega_1^2)(D^2 + 2\rho_2\omega_2 D + \omega_2^2)\alpha_r(t) = \omega_1^2\omega_2^2\alpha_r^*(t)$$

where D denotes the derivative operator. The parameters ($\rho_1 = 1$, $\rho_2 = 1$) of the command generator are kept fixed, but two sets of values ($\omega_1 = 3$, $\omega_2 = 3$ and $\omega_1 = 5$, $\omega_2 = 5$) are considered for simulation. The controller and adaptation gains are $\lambda = 5$, $c_1 = 20$ and $\gamma_1 = 1$, $\gamma_2 = 1$, respectively. The selected piecewise-constant command input (in degrees) is $\alpha_r^*(t) = 5$ for $t \in [0, t_s)$ and $\alpha_r^*(t) = 0$ for $t \geq t_s$ or $\alpha_r^*(t) = 10$ for $t \in [0, t_s)$ and $\alpha_r^*(t) = 0$ for $t \geq t_s$, where t_s is the switching time.

For case A, with adaptive control with slow and small α_r command, $\omega_1 = \omega_2 = 3$ and $\alpha_r* \in \{5, 0\}$ deg. A slow reference trajectory is generated by selecting the poles of the command generator at -3. The command input α_r^* switches at $t_s = 3$ s. The reference trajectory $\alpha_r(t)$ rises to 5 deg and then drops to 0 deg. Selected responses for the NCEA law are shown in Fig. 1. We observe smooth tracking of the angle of attack. The state variables remain bounded. The maximum tracking error is about 0.5 deg. The estimates $\hat{w}_i + \mu_i$ converge to some constant values. The control input δ remains within 21 deg, and $\Psi_s^T z$ converges to zero. Thus, the closed-loop trajectory is eventually confined to a manifold defined in Eq. (38), and therefore the adaptive controller recovers the performance of the deterministic controller.

The responses obtained using the CEA law are also plotted in Fig. 1. We observe accurate trajectory tracking. But the maximum value of the tracking error is 1.16 deg, which is more than twice the value for the NCEA law. The maximum value of the control magnitude for the CEA law is 19.90 deg. These peak control magnitudes of the NCEA and CEA laws differ by 1.1 deg. The CEA law has a slightly larger tracking error than that of the NCEA law, even at 10 s.

For case B, with adaptive control for fast but small α_r command, $\omega_1 = \omega_2 = 5$ and $\alpha_r* \in \{5, 0\}$ deg. For faster response, simulation is done using $\omega_1 = \omega_2 = 5$, but with the same command input α_r^* of case A. The poles of the command generator are at -5. The remaining parameters of the control system used for case A are retained. Selected responses for NCEA and CEA laws are shown in Fig. 2. We observe that the angle of attack closely follows the commanded trajectory. It is again observed that $\Psi_s^T z$ tends to zero. The maximum tracking error and control magnitude for the NCEA and CEA laws are 0.5072 and 21.0937 deg and 1.3487 and 20.5695 deg, respectively. Compared with the CEA law, the NCEA law gives a smaller tracking error (0.5072 deg). It is seen that the peak control magnitude for the NCEA law is only slightly larger than the peak value for the CEA law.

For case C, with adaptive control for slow but large α_r command, $\omega_1 = \omega_2 = 3$ and $\alpha_r* \in \{10, 0\}$ deg. For a larger α angle control, the command input is set as $\alpha_r^*(t) = 10$ for $t \in [0, 3)$ and then $\alpha_r^*(t) = 0$ for $t \geq 3$. The poles of the command generator are at -3, as in case A.

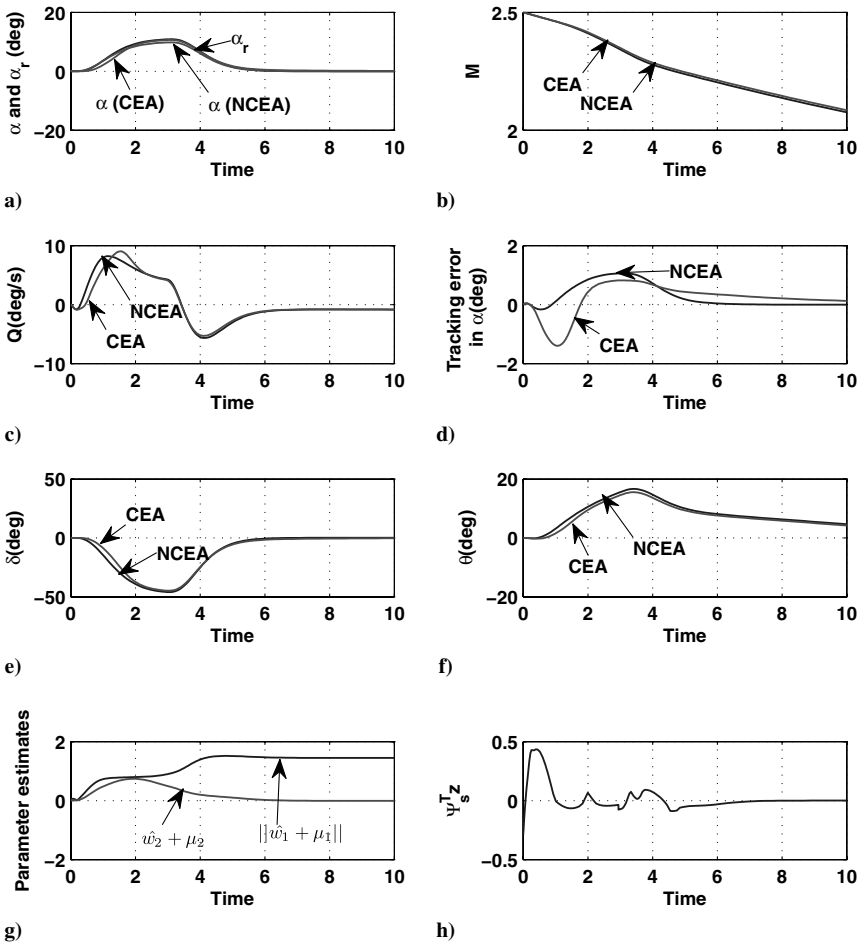

Fig. 3 Adaptive control for slow but large α_r command: $\rho_1 = 1$, $\rho_2 = 1$, $\omega_1 = 3$, $\omega_2 = 3$, and $\alpha_r* \in \{5, 0\}$ deg.

Selected responses for the NCEA and CEA laws are shown in Fig. 3. We observe that the angle of attack closely follows α_r and quickly attains close to 10 deg, as commanded, and then tends to zero. The peak value of the control input δ is larger than that of case A, as expected. It is again observed that $\Psi_s^T z$ tends to zero. The maximum tracking error and control magnitude for the NCEA and CEA laws are 1.0606 and 46.0002 deg and 1.3997 and 44.8372 deg, respectively. Compared with the CEA law, the tracking error for the NCEA law is again smaller, but the peaks in control magnitudes differ only by 1.2 deg.

For case D, with adaptive control for fast and large α_r command, $\omega_1 = \omega_2 = 5$ and $\alpha_r* \in \{10, 0\}$ deg. Simulation is done for a larger-angle-of-attack control using the faster command input of case C. The poles of the command generator are at -5. Selected responses for the NCEA and CEA laws are shown in Fig. 4. We observe that the angle of attack closely follows the reference trajectory. The control input δ is less than 48 deg for both laws. Similar to other cases, it is observed that $\Psi_s^T z$ tends to zero. The maximum tracking error and control magnitude for the NCEA and CEA laws are 1.1120 and 47.2608 deg and 1.5869 and 46.1040 deg, respectively. The tracking error for the NCEA law is again smaller than that for the CEA law, but the difference in peak magnitudes for the NCEA and CEA laws is small.

For case E, with nonadaptive control for slow but large α_r command, $\omega_1 = \omega_2 = 3$ and $\alpha_r* \in \{10, 0\}$ deg. To examine the advantage of adaptive control system, a nonadaptive feedback-linearizing control law is implemented. Based on Eq. (17), the feedback-linearizing nonadaptive control law is selected as $\delta = \text{sgn}(b_{03})M^{-2}u$, where

$$u = -\hat{w}_2[\Psi^T \hat{w}_1 - \ddot{\alpha}_r + \lambda\dot{\tilde{\alpha}}_r + c_1 s]$$

and $\hat{w}_1$ and $\hat{w}_2$ are offnominal values of w_1 and $w_2 = (1/b_1)$. These controller parameters remain constant for the nonadaptive control system. For a fair comparison, the control gains λ and c_1 used for the adaptive law are retained. It is interesting to note that the adaptive systems accomplish trajectory control even for the choice of control effectiveness gain $\hat{w}_2(0) = 0$. (For this choice, the nonadaptive system will have control input zero and, as such, obviously cannot accomplish trajectory control.)

Simulation is performed for 1) arbitrary perturbation within $\pm 10\%$ and 2) uniform perturbation of $\pm 10\%$. For arbitrary perturbation within $\pm 10\%$ of the actual values, one has

$$\hat{w}_1 = P_\Delta w_1, \qquad \hat{w}_2 = \Delta_4 w_2$$

where $\Delta_4 = 0.9$ or 1.1. The perturbation matrix P_Δ for uncertainty within $\pm 10\%$ is assumed to be

$$P_\Delta = \text{diag}\{\Delta_1, \Delta_2, \Delta_3, \Delta_1, \Delta_2, 1\}$$

where

$$\Delta_1 = [1, 1.1, 0.9, 1.1, 1], \qquad \Delta_2 = [0.9, 1, 1.1, 1, 0.9]$$
$$\Delta_3 = [1.1, 0.95, 1, 1.1, 1.01]$$

First, simulation is done for the slow command signal of case C for $\alpha_r = 10$ deg and $\Delta_4 = 0.9$. The selected responses are shown in Fig. 5. We observe that for this choice of perturbed parameters, the angle of attack has a maximum error of 0.6708 deg for 10 deg command, which is small compared with 1.1 deg obtained with the NCEA law (with large uncertainties, $\hat{w}_i(0) = 0$) (Fig. 3d), and maximum control input required is 37.41 deg.

Simulation is done for $\hat{w}_1 = P_\Delta w_1$ and $\hat{w}_2 = \Delta_4 w_2$, where $\Delta_4 = 1.1$. For this case, a larger tracking error of the magnitude

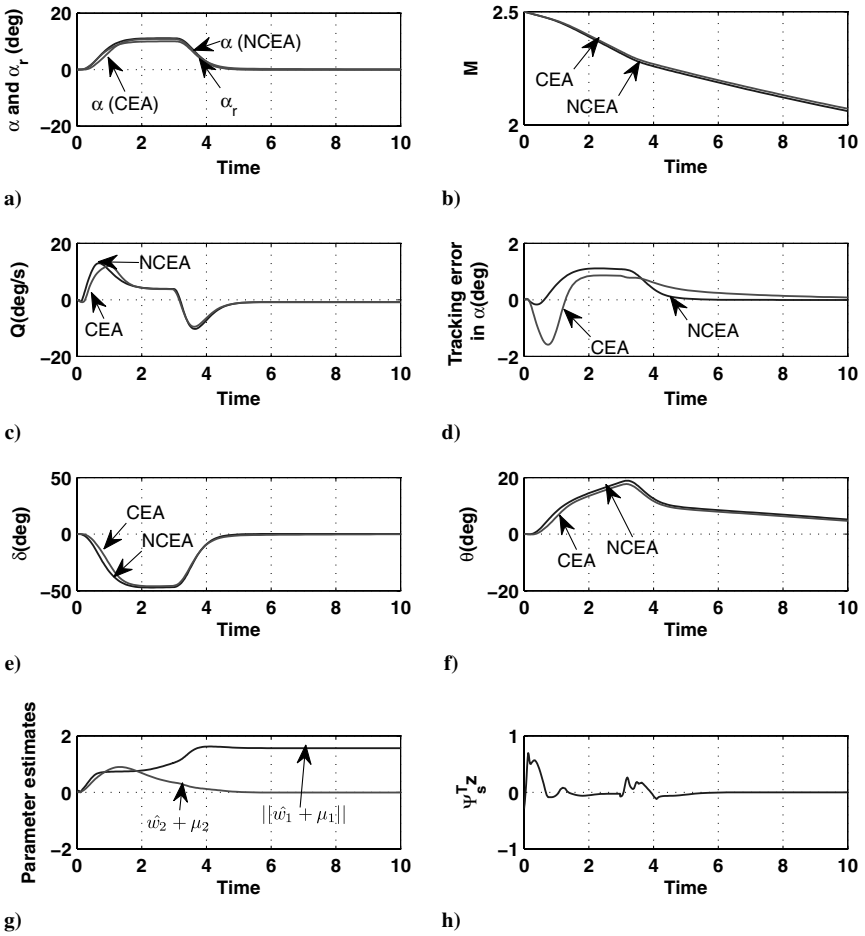

Fig. 4 Adaptive control for fast and large α_r command: $\rho_1 = 1$, $\rho_2 = 1$, $\omega_1 = 5$, $\omega_2 = 5$, and $\alpha_r* \in \{10, 0\}$ deg.

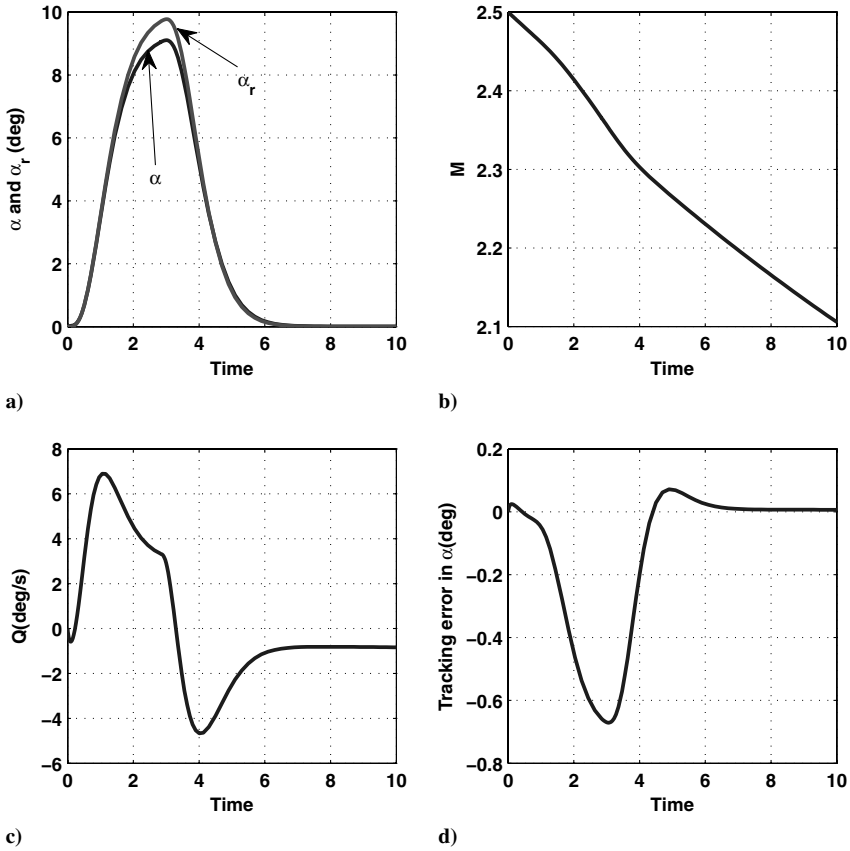

Fig. 5 Nonadaptive control for slow but large α_r command: $\rho_1 = 1, \rho_2 = 1, \omega_1 = 3, \omega_2 = 3, \hat{w}_1 = P_\Delta w_1, \hat{w}_2 = \Delta_4 w_2, \Delta_4 = 0.9$, and $\alpha_r* \in \{10, 0\}$ deg.

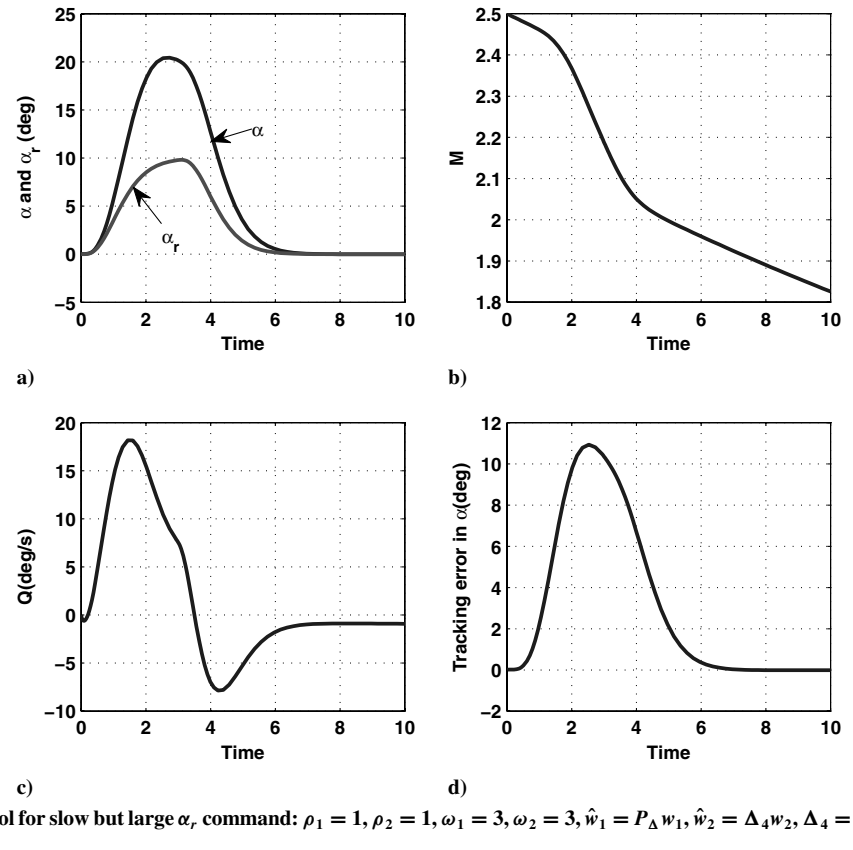

Fig. 6 Nonadaptive control for slow but large α_r command: $\rho_1 = 1, \rho_2 = 1, \omega_1 = 3, \omega_2 = 3, \hat{w}_1 = P_\Delta w_1, \hat{w}_2 = \Delta_4 w_2, \Delta_4 = 1.1$, and $\alpha_r* \in \{10, 0\}$ deg.

10.91 deg is observed for the 10 deg command. Responses are shown in Fig. 6. This error is quite large compared with the peak value of the NCEA law (Fig. 3d).

Now simulation is performed for the uniform perturbation of $\pm 10\%$. It is found that for $P_\Delta = 1.1 I_{26\times 26}$ and $\Delta_4 = 0.9$, the maximum tracking error is 0.58 deg, but for $P_\Delta = 0.9 I_{26\times 26}$ and $\Delta_4 = 0.9$, the tracking error is 3.6 deg. These results show that the tracking performance of nonadaptive law heavily depends on the values of the perturbed parameters. The responses in Figs. 5 and 6 are only for small uncertainty of $\pm 10\%$. For larger uncertainties, it is obvious that the performance of the nonadaptive law will further deteriorate. Therefore, for obtaining good tracking performance, adaptive law is quite useful.

Simulation results for different controller parameters and command inputs have been obtained. These results show that the designed NCEA law accomplishes smooth control of the angle of attack. Furthermore, for the chosen controller parameters, the tracking error for the NCEA law is smaller than that for the CEA law for each case. However, one must note that like any adaptive system, the transient performance of the NCEA and CEA system is highly dependent on the feedback and adaptation gains and the estimates $[\hat{w}_i(0)]$ of the unknown parameters. We have observed that for some other choices of controller gains, the NCEA law gives a larger tracking error than the CEA law, but compared with the CEA law, the advantages of the NCEA law described in Remarks 1 and 2 remain valid for each case. The gains of the control module and the adaptation gains of the estimator of the NCEA system can be independently chosen for shaping the response characteristics.

VI. Conclusions

In this paper, based on the immersion-and-invariance theory, a new adaptive longitudinal autopilot for control of a missile was designed. This design methodology gave a noncertainty-equivalent adaptive control system that has a modular structure consisting of a stabilizer (control module) and an estimator. The stability analysis for the control module and the identifier was performed separately using two distinct Lyapunov functions. This allowed flexibility in adjusting the rate of convergence of parameter estimation error independently. Using a composite Lyapunov function, it was then shown that in the closed-loop system, the angle-of-attack trajectory tracking error asymptotically converged to zero. A traditional certainty-equivalent control system was also designed. It was also shown that unlike the certainty-equivalent adaptive controllers, parameter estimates using the NCEA law will remain frozen for all future time if the estimation error attained zero value at any single instant. Moreover, the NCEA law accomplished regulation of the trajectories to a manifold on which the system recovered the performance of the deterministic controller. Simulation results showed accurate tracking of the angle of attack in spite of large parameter uncertainties. It was seen that for properly chosen feedback and adaptation gains, the NCEA controller gave a better tracking-error control performance than the CEA controller.

References

[1] Cloutier, J. R., Ever, J. H., and Feeley, J. J., "An Assessment of Air-to-Air Missile Guidance and Control Technology," *Proceedings of the American Control Conference*, Inst. of Electrical and Electronics Engineers, Piscataway, NJ, 1988, pp. 133–142.

[2] Williams, D. E., Friedland, B., and Madiwale, A. N., "Modern Control Theory for Design of Autopilot for Bank-to-Turn Missile," *Journal of Guidance, Control, and Dynamics*, Vol. 10, No. 4, 1987, pp. 378–386. doi:10.2514/3.20228

[3] Theodoulis, S., and Duc, G., "Missile Autopilot Design: Gain-Scheduling and the Gap Metric," *Journal of Guidance, Control, and Dynamics*, Vol. 32, No. 3, 2009, pp. 986–996. doi:10.2514/1.34756

[4] Shamma, J. S., and Cloutier, J. R., "Gain-Scheduled Missile Autopilot Design Using Linear Parameter Varying Transformations," *Journal of Guidance, Control, and Dynamics*, Vol. 16, No. 2, 1993, pp. 256–263. doi:10.2514/3.20997

[5] Tan, W., Packard, A. K., and Balas, G., "Quasi-LPV Modeling and LPV Control of Generic Missile," *Proceedings of the American Control Conference*, Inst. of Electrical and Electronics Engineers, Piscataway, NJ, 2000, pp. 3692–3896.

[6] Lin, C.-F., *Advanced Control Systems Design*, Prentice–Hall, Englewood Cliffs, NJ, 1994.

[7] Corey, S., and Khargonekar, P. P., "Stability Analysis of a Missile Control System with a Dynamics Inversion Controller," *Journal of Guidance, Control, and Dynamics*, Vol. 21, No. 3, 1998, pp. 508–515. doi:10.2514/2.4266

[8] Menon, P. K., and Ohlmeyer, E. J., "Integrated Design of Agile Missile Guidance and Autopilot Systems," *Control Engineering Practice*, Vol. 9, No. 10, 2001, pp. 1095–1106. doi:10.1016/S0967-0661(01)00082-X

[9] Menon, P. K., Iragavarapu, V. R., and Ohlmeyer, E. J., "Software Tools for Nonlinear Missile Autopilot Design," *AIAA Guidance, Navigation, and Control Conf.*, AIAA Paper 99-3975, Portland, OR, 1999.

[10] Ha, I.-J., and Chong, S., "Design of a CLOS Guidance Law Via Feedback Linearization," *IEEE Transactions on Aerospace and Electronic Systems*, Vol. 28, No. 1, 1992, pp. 51–63. doi:10.1109/7.135432

[11] Romano, J. J., and Singh, S. N., "I-O Map Inversion, Zero Dynamics, and Flight Control," *IEEE Transactions on Aerospace and Electronic Systems*, Vol. 26, No. 6, 1990, pp. 1022–1029. doi:10.1109/7.62254

[12] McFarland, M. B., and D'Souza, C. N., "Missile Flight Control with Dynamic Inversion and Structured Singular Value Decomposition," *AIAA Guidance, Navigation, and Control Conference*, AIAA, Washington, D.C., 1994, pp. 544–550.

[13] Wise, K. A., and Sedwick, J. L., "Nonlinear H_∞ Optimal Control for Agile Missiles," *AIAA Guidance, Navigation, and Control Conference*, AIAA, Washington, D.C., 1995, pp. 1295–1307.

[14] Mracek, C. P., and Cloutier, J. R., "Missile Longitudinal Autopilot Design Using the State-Dependent Riccati Equation Method," *Proceedings of the International Conference on Nonlinear Problems in Aviation and Aerospace*, Embry-Riddle Aeronautical Univ. Press, Daytona Beach, FL, 1996, pp. 387–396.

[15] Cloutier, J. R., and Stancebery, D. T., "Nonlinear Hybrid Bank-to-Turn/Skid-to-Turn Missile Autopilot Design," AIAA Paper 2001-4158, Aug. 2001.

[16] Xin, M., and Balakrishnan, S. N., "Missile Longitudinal Autopilot Design Using a New Suboptimal Nonlinear Control Method," *IEE Proceedings—Control Theory and Applications*, Vol. 150, No. 6, 2003, pp. 577–584. doi:10.1049/ip-cta:20030966

[17] Xin, M., and Balakrishnan, S. N., Stancebery, D. T., and Ohlmeyer, E. J., "Nonlinear Missile Autopilot Design with θ-D Technique," *Journal of Guidance, Control, and Dynamics*, Vol. 27, No. 3, 2004, pp. 406–417. doi:10.2514/1.1217

[18] Thukral, A., and Innocenti, M., "A Sliding Mode Missile Pitch Autopilot Synthesis for High Angle of Attack Maneuvering," *IEEE Transactions on Control Systems Technology*, Vol. 6, No. 3, 1998, pp. 359–371. doi:10.1109/87.668037

[19] Salamci, M. U., and Ozgoren, M. K., "Sliding Mode Control with Optimal Sliding Surfaces for Missile Autopilot design," *Journal of Guidance, Control, and Dynamics*, Vol. 23, No. 4, 2000, pp. 719–727. doi:10.2514/2.4588

[20] Bhat, M. S., and Powly, A. A., "Variable Structure Controller Design with Application to Missile Tracking," *Journal of Guidance, Control, and Dynamics*, Vol. 24, No. 4, 2001, pp. 859–862. doi:10.2514/2.4790

[21] Shkolnikov, I. A., and Shtessel, Y. B., "Robust Missile Autopilot Design Via High-Order Sliding Mode Design," AIAA Paper 2000-3968, Aug. 2000.

[22] Shima, T., Idan, M., and Golan, O. M., "Sliding-Mode Control for Integrated Missile Autopilot Guidance," *Journal of Guidance, Control, and Dynamics*, Vol. 29, No. 2, 2006, pp. 250–260. doi:10.2514/1.14951

[23] Krause, J., and Stein, G., "A General Adaptive Control Structure with a Missile Application," *Proceedings of the American Control Conference*, Inst. of Electrical and Electronics Engineers, Piscataway, NJ, 1988, pp. 561–566.

[24] Kamen, E. W., Bullock, T. E., and Song, C., "Adaptive Control Applied to Missile Autopilots," *Proceedings of the American Control Conference*, Inst. of Electrical and Electronics Engineers, Piscataway, NJ, 1988, pp. 555–560.

[25] Cao, C., and Hovakimyan, N., "L_1 Adaptive Output-Feedback Controller for Non-Strictly-Positive-Real Reference Systems: Missile

Longitudinal Autopilot Design," *Journal of Guidance, Control, and Dynamics*, Vol. 32, No. 3, 2009, pp. 717–726.
doi:10.2514/1.40877

[26] Fu, L.-C., Chang, W.-D., Yang, J.-H., and Kuo, T.-S., "Adaptive Robust Bank-to-Turn Missile Autopilot Design Using Neural Networks," *Journal of Guidance, Control, and Dynamics*, Vol. 20, No. 2, 1997, pp. 346–354.
doi:10.2514/2.4044

[27] Lin, C. C., and Chen, F. C., "Improving Conventional Longitudinal Autopilot Using Cerebellar Articulation Controller Neural Networks," *Journal of Guidance, Control, and Dynamics*, Vol. 26, No. 5, pp. 711–718.
doi:10.2514/2.5125

[28] Astofi, A., and Ortega, R., "Immersion and Invariance: A New Tool for Stabilization and Adaptive Control of Nonlinear Systems," *IEEE Transactions on Automatic Control*, Vol. 48, No. 4, 2003, pp. 590–606.
doi:10.1109/TAC.2003.809820

[29] Karagiannis, D., and Astolfi, A., "Nonlinear Adaptive Control of Systems in Feedback Form: An Alternative to Adaptive Backstepping," *IFAC Symposium on Large Scale Systems: Theory and Applications*, Elsevier IFAC, Amsterdam, 2004, pp. 71–76.

[30] Astolfi, A., Karagiannis, D., and Ortega, R., *Nonlinear and Adaptive Control with Applications*, Springer–Verlag, London, 2008, pp. 276–309.

[31] Seo, D., and Akella, M. R., "High-Performance Spacecraft Attitude-Tracking Control Through Attracting-Manifold Design," *Journal of Guidance, Control, and Dynamics*, Vol. 31, No. 4, 2008, pp. 884–891.
doi:10.2514/1.33308

[32] Lee, K. W., and Singh, S. N., "Immersion- and Invariance-Based Adaptive Control of a Nonlinear Aeroelastic System," *Journal of Guidance, Control, and Dynamics*, Vol. 32, No. 4, 2009, pp. 1100–1110.
doi:10.2514/1.42475

[33] Ionnou, P. A., and Sun, J., *Robust Adaptive Control*, Prentice–Hall, Upper Saddle River, NJ, 1996.